Measurements of the Fluorescence Light Yield in Electromagnetic Showers

K. Reil, P. Chen, C. Field, C. Hast, R. Iverson, J.S.T. Ng, A. Odian, H. Vincke, and D. Walz
SLAC, Stanford, CA 94025, USA
J. Belz, A. Goldammer, and D. Guest
University of Montana, Missoula, MT, 59812, USA
D.R. Bergman, S. Cavanaugh, L. Perera, S. Schnetzer, G.B. Thomson, and A. Zech
Rutgers University, Piscataway, New Jersey, 08854, USA
Z. Cao, P. Huentemeyer, C.C.H. Jui, E.C. Loh, K. Martens, J.N. Matthews, J.D. Smith, P. Sokolsky, R.W. Springer, and S.B. Thomas
University of Utah, Salt Lake City, UT, 84112, USA
F.Y. Chang, C.C. Chen, C.W. Chen, M.A. Huang, W-Y. P. Hwang, and G.-L. Lin
Center for Cosmology and Particle Astrophysics (CosPA), Taiwan

The two most common methods of determining the energy of an ultra high energy cosmic ray (UHECR) are ground arrays and fluorescence telescopes. Ground array detectors determine energy by sampling the number of shower particles arriving at the surface of the earth. In general, the more particles, the higher the energy. Fluorescence telescopes, on the other hand, determine the energy by measuring the number of ultraviolet photons produced by the electromagnetic shower produced in the atmosphere. The number of photons is related to the number of particles in the shower by the fluorescence yield (measured in photons per meter per charged particle). The Akeno Giant Air Shower Array (AGASA) and the High Resolution Flys Eye (HiRes) are the current world leading ground array and fluorescence detectors, respectively. Recent results from the two experiments indicate a significant discrepancy in the flux of cosmic rays as a function of energy[1–3]. This indicates that there may be a systematic offset in energy determination in the two techniques.
The FLuorescence in Air from SHowers (FLASH) experiment is an effort to reduce the systematic uncertainty in energy determination for fluorescence detectors by making an improved measurement of the fluorescence yield. This work is intended to add to the prior work of Bunner, Kakimoto *et al.* and Nagano *et al.*[4–7]. We report on the current status of the experiment.

1. Introduction

When a UHECR interacts with the earths atmosphere it creates an extensive air shower. This shower consists of, for the most part, electromagnetic subshowers. The charged electromagnetic particles interact with the air molecules pushing them (primarily N_2) into excited states. In turn, ultraviolet (UV) light is emitted upon deexcitation. In the FLASH experiment, we measure the number of UV photons produced per charged particle per meter. This fluorescence yield sets the energy scale for fluorescence technique UHECR detectors.

The FLASH experiment consists of three distinct experimental phases. First, in a proof in principle test beam experiment (T-461), we measured the total fluorescence yield. Second, in the "thin target" run of the FLASH experiment (E-165) we remeasured the total fluorescence yield and resolved the spectral shape of the fluorescence light. Finally, during the "thick target" run, we measured the fluorescence yield as a function of shower depth.

All three phases of this experiment shared a common location in the Final Focus Test Beam (FFTB) facility at SLAC. Electrons were delivered to the FFTB with energy of 28.5 GeV with 10^7 to 10^{10} electrons per pulse depending upon the experimental configuration and requested intensity.

2. Total Fluorescence Yield: T-461

In June of 2002, a test experiment (T-461) was conducted. The total yield was measured by observing the produced fluorescence light through a band pass filter (300-400 nm). The total yield was measured in pure nitrogen and various nitrogen/oxygen mixtures, including dry air.

2.1. Experimental Apparatus

The T-461 chamber consisted of a six inch diameter tube with (thickness) beam windows on the up and downstream sides. The light produced in the chamber was observed via baffled optical arms. The first baffle defined the observed track length. Figure 1 shows the full FLASH thin target chamber. The T-461 chamber is identical to this chamber the exception of an additional filter wheel and a concentric tube to define observed track length. The electron beam, in this figure, travels upward and through the chamber. The produced fluorescence light travels down the optical arms, through a band pass filter, reflects off a 45^o mirror and into a Photonis XP 3062 PMT. An opposing optical arm contained an UV LED which was triggered out of time with the electron beam to track PMT stability.

Presented at 22nd Texas Symposium On Relativistic Astrophysics, 12/13/2004-12/17/2004, Stanford, CA, USA

Work supported in part by the Department of Energy contract DE-AC02-76SF00515

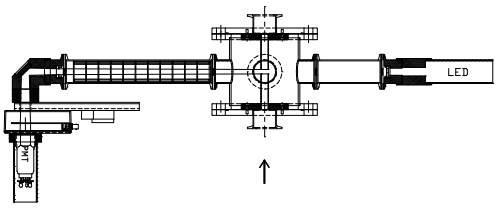

Figure 1: FLASH Thin Target Chamber

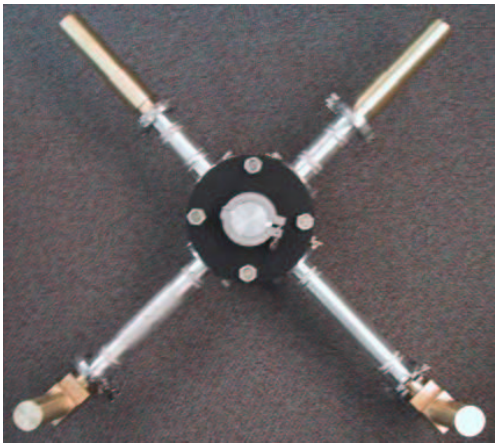

Figure 2: T-461 Target Chamber

The system was symmetric along an east-west electron beam. The two optical arms and two LED calibration arms are labeled as north and south based on their geometry around the electron beam. Figure 2 shows a photo, looking in the downstream direction, of the T-461 system as it would have been installed.

A gas control system was attached to the vessel and consisted of two gas inputs, a vacuum reservoir and pump and flow control valves on both input and output.

Background noise from radiation is inherent in the FFTB environment. A reference background signal was determined by measuring the signal produced in ethylene, a non fluorescing gas. Changes in the background noise level were tracked using two "blind" PMTs that were installed in black photographer bags adjacent to the two signal PMTs.

2.2. Data Collection

The PMT signals were read out using a 2249W ADC and the beam charge was determined using a SLAC toroid. Pressure, temperature and PMT high voltage were all recorded at a rate of around 0.5 Hz using a smart analog monitor (SAM) unit[8].

2.3. Analysis

In order to measure the fluorescence yield,

$$Y = \frac{\gamma}{me^-} \tag{1}$$

several calibrations were required. First, the number of electrons exciting the fluorescence had to be measured. This was accomplished using a SLAC toroid. During a later data run, this toroid was calibrated with a specially designed and well calibrated toroid. This cross calibration provides a measure of beam charge to around 10% uncertainty.

The optical acceptance was calculated from the geometry and the responsivity of the PMTs were cross calibrated with a hybrid photo-diode using the HiRes spectrophotometer system in Utah[9]. The optical acceptance, and gain were also calibrated to approximately 10%.

Assuming the spectral shape provided by Bunner[4] the total fluorescence yield was determined to be $4.93 \pm 0.64 \frac{\gamma}{e^- m}$ in dry air. In nitrogen the yield was measured to be $36.1 \pm 4.65 \frac{\gamma}{e^- m}$. Details of this analysis were reported previously and a full report incorporating the recent cross calibration of toroids is expected shortly[10].

2.4. Conclusions

The total fluorescence yield in dry air and pure nitrogen were measured at the $\sim 15\%$ level. However, no information on the spectral distribution of fluorescence light was obtained during the test run.

3. Fluorescence Yield: E-165 Thin Target

In September 2003, thin target data was taken. The apparatus is shown in Figure 1. The main modification from T-461 was the addition of a filter wheel immediately after the 45^o mirror in the optical arm. Additionally, a one centimeter observation length was defined inside the main chamber by a $(1\ cm)$ gap in a concentric cylinder with a radius of 5/8".

A set of narrow band filters were used to measure the strength of the various fluorescence lines. Again, observations were made using the unshowered FFTB electron beam. In addition, to the narrow band filter observations, the total fluorescence yield was remeasured using a band pass (300-400 nm) and an open (sans) filter setting.

A black filter setting was used to measure background levels. After every 8 filters settings, the black filter was reinserted to track changes in background levels. Additionally, changes in background levels were also tracked using two "blind" PMTs and a scintillator/PMT counter.

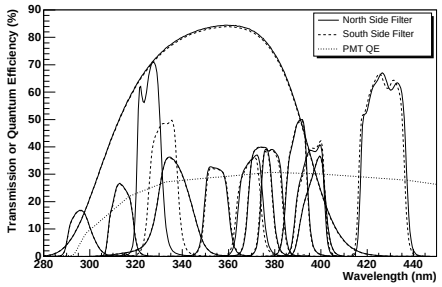

Figure 3: FLASH Filter Transmissions and nominal PMT QE

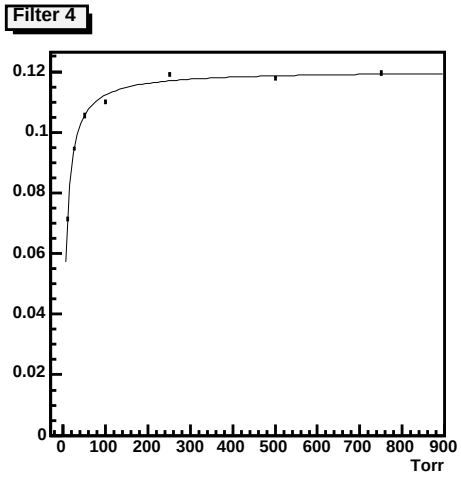

Figure 4: Yield vs Pressure for the 337 nm narrow band filter.

Again, pressure, temperature and PMT high voltage were recorded at approx 0.5 Hz.

3.1. Data

Data was collected at 8 pressures (5, 10, 25, 50, 100, 250, 500 and 750 Torr) for all 15 filter settings using pure nitrogen, dry air and humid filtered air from the atmosphere at SLAC. 5000 or more beam events were collected at 10 Hz for each setting. Figure 4 shows a typical yield vs pressure curve for the 337 nm line in air. The expected plateau in the yield at higher pressures is observed as expected[4].

3.2. Analysis

The fluorescence yield for a given filter (i) is determined by

$$Y_i = \frac{\gamma_i}{me^-} \tag{2}$$

Both of the signal PMTs recorded a total number of ADC counts (N_{ADC}) for each beam event. The N_{ADC} from the fluorescence signal is determined by

$$N_{ADC} = N_{measured} - N_{pedestal} - N_{background} \tag{3}$$

The ADC pedestal count rate ($N_{pedestal}$) was measured using a prescaled, out of time, ADC gate. The background rate was determined in one of two ways:

$$N_{background} = R_j \times N_{BG} \tag{4}$$

where R_j is the ratio of the counts in the signal tube to the counts in one of the three background counters when the black filter is in place and N_{BG} is the number of counts observed in the background counter. There were three background counters used, two blind tubes and a scintillator/PMT counter.

Additionally, under the observed assumption that background levels were constant over large periods of time, the average signal observed in the signal PMT during a black filter run could be used as a measure of the background. In practice the background was, in fact, sufficiently stable.

Once the number of ADC counts is known, a calibration constant (C_{calib}) is applied to convert ADC counts to photons per meter. This calibration constant is determined using the Rayleigh scattering of laser light fired along the same path as the electron beam[13, 14].

The yield is finally determined by dividing by the measured number of electrons.

$$Y_i = \frac{N_{ADC} * C_{calib}}{N_{e^-}} \tag{5}$$

3.3. Results

To determine the strength of various spectral lines, the measured number of photons can be divided by the filter transmission efficiency and the PMT quantum efficiency. Figure 5 shows the resulting spectrum at atmospheric pressure in dry air.

However, this simple measure does not include the effects from cross talk between filters. A simple Monte Carlo corrects for this by adjusting the line strengths (of lines located at the peak of the various filter transmissions) until the adjusted spectrum correctly predicts the observed signals in all narrow band filters. Figure 6 shows the spectrum produced in this manner. The effect of this correction reduces the determined total yield since a single emission band, producing signal in multiple filters, is accounted for. Examination of Figure 6 also shows that we are unable to resolve where light is emitted in two overlapping filters (375 or 380 nm, for example).

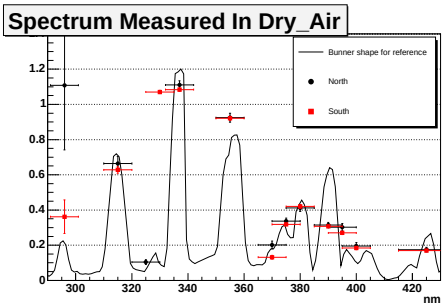

Figure 5: Spectrum at Atmospheric pressure in Dry Air without Cross Talk Corrections

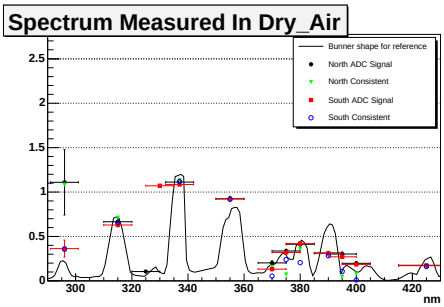

Figure 6: Spectrum at Atmospheric pressure in Dry Air Consistent with All Measured Signals

In both prior cases, it is assumed that all light is emitted at wavelegths corresponding to the peak of the fitler transmission. While attempts were made to use a narrow band filter near all known lines, the location of the emission is not always at the maximal transmission of the filter. When corrections are made for this, the determined yield will increase since more light is required to produce the same signal when the band is located away from the peak filter transmission.

To help resolve the true wavelengths of emission, a spectrograph system was used to measure the spectral shape of the fluorescence light. This system consisted of a separate thin target chamber with a single optical arm leading to a spectrograph. Figure 7 show the spectrum measured in dry air at atmospheric pressure. The measured spectrum can then be normalized to give the correct total signal as measured with the wide band or open filter settings. A larger total yield is always found in this case.

Work is in progress to study the effects of various spectral shape assumptions. Additionally, the calibration work for the thin target effort is almost concluded. A full report can be expected soon.

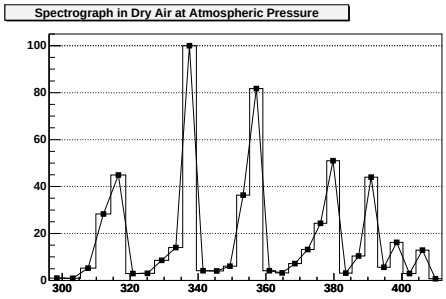

Figure 7: Spectrum at Atmospheric pressure in Dry Air measured by the Spectrograph

4. Fluorescence in Showers: E-165 Thick Target

In addition to checking the fluorescence yield, we wished to confirm that fluorescence light was emitted proportionally to shower size at all shower depths. To do so the electron beam was showered with various radiation lengths (RL) of alumina (Al_2O_3) with shower maximum occurring at approximately 6 RL.

In addition to measuring the longitudinal development of the shower, a first attempt to measure the lateral distribution of particles was also made.

4.1. Experimental Setup

The thick target mode of the experiment consisted of a $(50\ cm)^2$ optical chamber located behind varying thicknesses of showering material. In the nominal beam center of the optical box were two beam windows made of aluminum foil and covered with flock paper inside the chamber.

An optical arm with two 45^o degree mirrors viewed the 4 cm length of the optical chamber. The optical arm contained the two doglegs in order to prevent direct radiation from hitting the PMTs. A total of six PMTs were used, two were "blinded" to track background levels and four observed the fluorescence volume. The interior of the optical box and optical arms were covered with black flock paper and were baffled with 1 cm baffles.

The showering material, consisting of alumina bricks, was located inside of remotely movable aluminum boxes. There were four boxes of alumina, three containing 4 RL of material and one with 2 RL as shown in Figure 8. Eight combinations were used to provide total shower depths from 0 to 14 radiation lengths in 2 radiation length steps.

The nominal beam charge during thick target running was reduced to approximately 1% of the thin target value (to $10^7\ e^-$ per pulse). This was, in part, to satisfy the accelerator safety design requiring that less then 1% loss of the full FFTB could be lost in the tunnel.

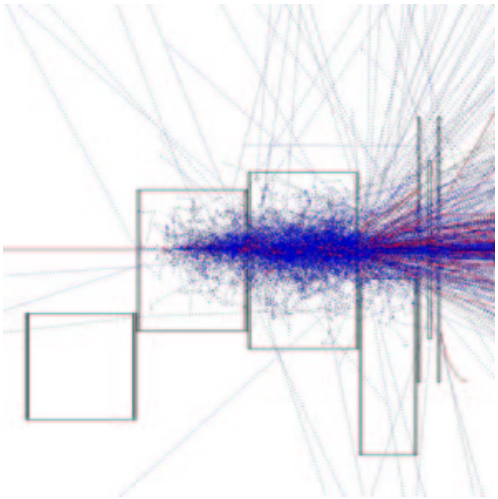

Figure 8: Alumina Target

In addition to the optical system, several additional detectors were used.

4.2. Additional Apparatus

Immediately downstream of the optical box, one or more of three detectors could be installed. These detectors included an ion chamber which measured the flux of shower particles, a CCD camera with a scintillating screen to image the shower spot and a four diamond detector which counted particles while scanning the lateral profile.

An ion chamber was used to track shower size as a function of shower depth. This allowed us to compare the measured fluorescence signal and the number of shower particles simultaneously. This removed some of our dependence on predicted shower size from Monte Carlo codes such as EGS and GEANT[11][12]. Additionally, the measured shower size could provide a cross check on these shower simulation codes.

A scintillating screen was mounted over the exit window of the optical chamber. The produced scintillation light was reflected with mirrors twice before entering a CCD camera. Figure 9 shows the lateral profile of the shower at 6 RL. The scintillation screen had a very long decay time making the image an average of many showers.

Finally, four diamond detectors were mounted on an XYZ mover. The intensity of charged particles was measured at 4 lateral distances and scanned in 1 cm steps. Figures 10 shows the measured lateral profile at 6 RL. At the time of this proceedings the cross calibration of the diamonds was still at a preliminary stage.

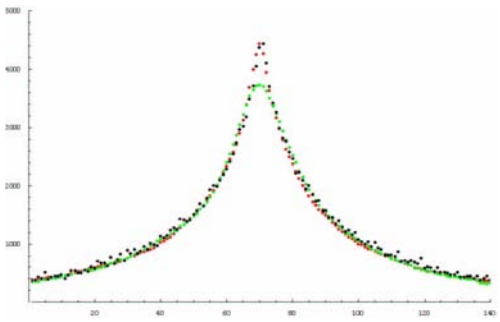

Figure 9: Lateral Profile as Measured by the CCD Camera

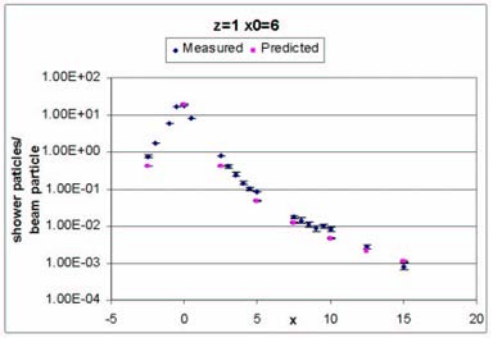

Figure 10: Lateral Profile as Measured Diamond Detectors

4.3. Thick Target Results

The (almost complete) removal of the 2 RL alumina box created an air gap with some shadowing in the the $4, 8, 12$ RL data. For example, Figure 8 shows the 8 RL case. Monte Carlo modeling was needed to correct for this effect. With corrections applied, Figure 11 shows the measured shower development using both the ion chamber and the fluorescence light signal. Additionally, the shower curve predicted by GEANT is included with a fit to the functional form $Cx^b e^{-ax}$. All three curves are normalized to have the same total area.

Work is ongoing to improve our analysis of this data.

5. Summary

The total fluorescence yield was measured measured to be 4.93 ± 0.64 in T-461. In the E-165 thin target run the spectral distribution of the fluorescence light was measured using both a spectrograph system and narrow band filters. Early indications are that while the fine details of the spectrum requires further study, no large discrepancy from previous works was seen in the measured fluorescence yield.

The fluorescence yield was shown to follow the shower development within errors as was expected.

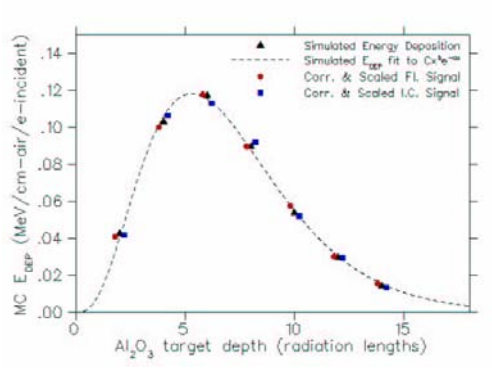

Figure 11: Shower Development Curve including Fluorescence and Ion Chamber Signals. Comparison with GEANT

Additionally, the lateral distribution of particles in the electromagnetic showers was measured. Work is ongoing.

Acknowledgments

The authors wish to thank the SLAC staff for their support of our experiment. This work was supported by Department of Energy contract DE-AC02-76SF00515. Additionally, FLASH was supported by the NSF and by the HiRes calibration budget.

References

[1] M. Takeda *et al.*, Astrophys. J. 522 (1999) 225.
[2] M. Takeda *et al.*, Phys. Rev. Lett. **81** (1998) 1163.
[3] R. Abassi *et al.*, Phys. Rev. Lett. **92** (2004) 151101.
[4] A. N. Bunner, Ph. D. thesis (Cornell University) (1967).
[5] F. Kakimoto, E. C. Loh, M. Nagano, H. Okuno, M. Teshima, S. Ueno, Nucl. Intrum. Methods Phys. Res., **A372** (1996) 244.
[6] M. Nagano, K. Kobayakawa, N. Sakaki, K. Ando, Astropart. Phys. **20** (2003) 293.
[7] M. Nagano, K. Kobayakawa, N. Sakaki, K. Ando, Astropart. Phys. **22** (2004) 235.
[8] http://www.slac.stanford.edu/grp/cd/soft/wwwman/hard.www/chapter42.html
[9] http://www-rccn.icrr.u-tokyo.ac.jp/icrc2003/PROCEEDINGS/PDF/228.pdf
[10] http://www-rccn.icrr.u-tokyo.ac.jp/icrc2003/PROCEEDINGS/PDF/211.pdf
[11] W. R. Nelson, H. Hirayama, and D. W.O. Rogers, SLAC-Report-265 (December 1985).
[12] R. Brun *et al.*, GEANT3 User's Guide, CERN DD/EE/84-1.
[13] M. Fukushima, N. Sakurai, L. Wiencke, http://www.physics.utah.edu/∼wiencke/c-rays/ppt/c-rays.html
[14] A. Bucholtz, Appl. Opt. **34** (1995) 2765-2773.